JOURNAL OF VIROLOGY, July 2006, p. 7028–7036 Vol. 80, No. 14
0022-538X/06/$08.00+0 doi:10.1128/JVI.00478-06

Rapid Pathogenesis Induced by a Vesicular Stomatitis Virus Matrix Protein Mutant: Viral Pathogenesis Is Linked to Induction of Tumor Necrosis Factor Alpha

Jean Publicover,[1,2] Elizabeth Ramsburg,[2]† Michael Robek,[2] and John K. Rose[2]*

Section of Microbial Pathogenesis[1] and Department of Pathology,[2] Yale University School of Medicine, New Haven, Connecticut 06510

Received 7 March 2006/Accepted 27 April 2006

Vesicular stomatitis virus (VSV) matrix (M) protein blocks host mRNA export from the nucleus and thereby inhibits interferon induction in infected cells. M mutants with mutations of methionine 51 (M51) lack this shutoff function. We examined pathogenesis of a VSV M mutant with a deletion of M51 (VSVΔM51) after intranasal infection of BALB/c mice and found an unexpected phenotype. Mice that received VSVΔM51 experienced a more rapid but overall less severe weight loss than mice that received the recombinant wild-type VSV (rwtVSV). Rapid weight loss was not explained by faster initial replication because VSVΔM51 replication was controlled faster than rwtVSV replication in the lungs and did not spread systemically like rwtVSV. This faster control of VSVΔM51 correlated with a more rapid induction of interferon in the lung. Because tumor necrosis factor alpha (TNF-α) is associated with weight loss, we examined TNF-α induction in mice infected with rwtVSV or VSVΔM51. We found more-rapid induction of TNF-α by the mutant at early times after infection, while rwtVSV induced more TNF-α later in infection. This result suggested that TNF-α induction might explain both the rapid weight loss caused by the mutant and the overall greater weight loss caused by the rwtVSV. Using TNF-α knockout mice (C57BL/6 background), we showed that weight loss following rwtVSV infection was greatly reduced in the absence of TNF-α. Although the rapid weight loss caused by VSVΔM51 was less pronounced in C57BL/6 mice, it was eliminated in the absence of TNF-α. These results indicate a role for TNF-α in the pathogenesis of VSV.

In a viral infection, innate immune responses such as synthesis of interferons can result in control of viral replication and establishment of strong adaptive immune responses. In order to ensure successful infections, many viruses have evolved mechanisms to block innate immune responses (see reference 31 for a review). Replication of vesicular stomatitis virus (VSV), an enveloped, negative-strand RNA virus, is very sensitive to inhibition by interferon alpha (IFN-α) and IFN-β. To overcome this sensitivity, the VSV matrix protein (M), a major structural protein of the virus, binds to a nuclear pore protein, designated Nup98, through the mRNA shuttling factor Rae1 and shuts off mRNA export from the nucleus, thereby preventing interferon induction in infected cells (4). The N-terminal 77 amino acids of the 229-amino-acid M protein are sufficient to inhibit mRNA transport, and a mutation or deletion of methionine residue 51 (M51) abolishes this inhibiting activity (15, 26, 30).

VSV infection causes disease in cattle (see reference 3 for a review) but also naturally infects a wide variety of mammals, including mice, in areas of enzootic disease (27). VSV given intranasally (i.n.) to mice is able to replicate in the lungs, establish a transient viremia, and also infect other organs before it is cleared (18, 19). Infection of mice with recombinant wild-type VSV (rwtVSV) results in severe weight loss of up to 20% of preinfection body weight, which occurs between days 2 and 5 following infection. This weight loss is a convenient measure of VSV pathogenesis (16, 18–20). VSV mutants that are attenuated for growth in culture cause reduced weight loss correlated directly with their ability to grow in culture (16, 19). Because we are studying the use of attenuated VSVs as vaccine vectors, we were particularly interested in examining specific, highly attenuated VSV mutants, such as the M51 mutant. This mutant is known to be less pathogenic than wild-type VSV (26). This reduction in pathogenesis is apparently due to failure to inhibit interferon synthesis in infected cells, resulting in early, high-level synthesis of IFN-α in the infected animals. Surprisingly, we found that this mutant induced a much more rapid weight loss in BALB/c mice than rwtVSV during the first 24 h after intranasal delivery, although the total weight loss was less severe than that eventually induced by rwt virus. We have determined that this rapid weight loss as well as the weight loss seen later in VSV infection can at least in part be explained by an immunopathology related to synthesis of the cytokine tumor necrosis factor alpha (TNF-α).

MATERIALS AND METHODS

Plasmid construction and virus recovery. The deletion of the codon for methionine 51 in the VSV matrix protein gene (ΔM51) was initially generated in the plasmid DNA template pVSVΔG-L, which has a deletion of the VSV G and L genes (18). The primers 5′CAAATCCTAT TTTGGAGTTG ACGAGGACAC CTATGATCCG AATCAATTAAG3′ (forward primer) and 5′CCTAATTGAT TCGGATCAT AGGTGTCCTCG TCAACTCC AAAATAGGATTTG 3′ (reverse primer) were used for mutagenesis carried out with a Stratagene QuikChange kit according to the manufacturer's instructions and 25 ng of template. Two microliters of PCR product was transformed into *Escherichia coli*

* Corresponding author. Mailing address: Department of Pathology, Yale University School of Medicine, 310 Cedar St. (LH 315), New Haven, CT 06510. Phone: (203) 785-6794. Fax: (203) 785-6127. E-mail: john.rose@yale.edu.

† Present address: Human Vaccine Institute, Duke University Medical Center, Durham, NC 27710.

DH5α cells. Plasmids prepared from colonies were purified, and the 3-nucleotide M51 deletion was confirmed by DNA sequencing (Yale Keck Sequencing Facility). To place this M51 deletion in the full-length VSV plasmid, pVSVΔG-L-ΔM51 was digested with XbaI and MluI to release the M gene containing the mutation. This fragment was then ligated into the full-length VSV plasmid pVSVXN2 (24) or pVSVEnvG (8), which had been digested with XbaI and MluI to release the wild-type matrix gene. The plasmids derived from the ligations were designated pVSVΔM51XN2 and pVSVΔM51EnvG. The correct plasmid structure was confirmed by restriction enzyme digestion. DNA sequencing was performed to confirm the structures of the M51 deletion and EnvG genes (Yale Keck Facility).

VSVΔM51 (the VSV M mutant with a deletion of M51) and VSVΔM51-EnvG (VSV-EnvG mutant with a deletion of M51) were recovered using a protocol previously described (10, 16). Recovered virus supernatants were filtered through a 0.1-μm filter, and stocks were grown from individual plaques and stored at −80°C. These stocks along with previously described stocks of rwtVSV (10) and VSV-EnvG (8) (rwtVSV expressing human immunodeficiency virus [HIV] Env with its cytoplasmic domain replaced by the VSV G cytoplasmic domain) were grown on BHK-21 cells, and titers were determined.

Metabolic labeling and SDS-PAGE. Cells were metabolically labeled as described previously (16). Briefly, one million BHK cells were infected with VSV recombinants for 5 h and then labeled for 1 h with 100 μCi of [^{35}S]methionine. Cell lysates were fractionated by sodium dodecyl sulfate-polyacrylamide gel electrophoresis (SDS-PAGE) (10% acrylamide), and proteins were visualized using autoradiography.

Inoculation of mice. Six- to eight-week-old female BALB/c mice were ordered from Charles River Laboratories. Six-week-old female TNF-α knockout mice (B6;129s6-Tnf$^{tm1GKl/J}$) were ordered along with age/sex-matched C57BL/6 mice from Jackson Laboratories. All mice were housed in microisolater cages in a biosafety level 2-equipped facility and were kept for 1 week before experiments were initiated. Virus inocula (total of 10^6 PFU/mouse) were diluted in serum-free Dulbecco's modified Eagle's medium (DMEM) and given in a final volume of 25 μl for i.n. administration or 50 μl for intramuscular (i.m.) administration. Virus was administered via the intranasal route after light anesthesia. Intramuscular injections were administered in the right hind leg. The Institute for Animal Care and Use Committee of Yale University approved of all animal experiments done in this study.

Tetramer assay. A tetramer assay was performed with fresh splenocytes as previously described (16). Cells that were Env tetramer positive, activated (CD62L^{lo}), and CD8 positive were identified using flow cytometry. In parallel, rwtVSV-vaccinated animals were used to determine background levels of tetramer binding.

Organ and plasma preparation and titers. At the appropriate time postinfection, mice were either bled by cardiac puncture to obtain plasma or perfused using sterile phosphate-buffered saline (PBS). Plasma was immediately centrifuged at 6,000 rpm in a TOMY centrifuge for 10 min, and supernatants were collected, aliquoted, and frozen at −80°C. Perfusions were performed by nicking the right atrium and flushing sterile PBS through the left ventricle. Following the whole-body perfusion, the lungs and liver were removed, divided in two, weighed, and immediately frozen in liquid nitrogen. Organs were then transferred to −80°C. For titration of virus from organs, half of each organ was added to serum-free DMEM and disrupted using a probe homogenizer (PowerGen 125; Fisher Scientific). After homogenization, the organ was immediately centrifuged to remove cell debris and supernatants were frozen in aliquots at −80°C. Determination of titers for both plasma and organ supernatants was performed with BHK cells. For plasma and lung supernatants, the sensitivity of the titer assay was 5 PFU/ml or 25 PFU/g, respectively (see Fig. 3A and B). For liver supernatants, the sensitivity of the titer assay was 250 PFU/g (see Fig. 3C).

IFN-α ELISA. Lung supernatants and plasma obtained as described above were used for an IFN-α enzyme-linked immunosorbent assay (ELISA) adapted from a previously described assay (11). Briefly, a flat-bottomed plate was coated with rat anti-mouse IFN-α (monoclonal antibody F-18; HyCult Biotechnology) in carbonate buffer (33.5 mM Na_2CO_3, 0.1 M $NaHCO_3$ [pH 9.5]) overnight at 4°C. Plates were then washed with wash buffer (0.5% Tween in PBS) three times and blocked with 10% fetal bovine serum in PBS for 2 h at room temperature. Plates were washed twice and incubated with lung supernatants or plasma diluted in block solution. Additionally, a recombinant mouse IFN-α standard (HyCult Biotechnology) was used at concentrations ranging from 2,000 pg/ml to 2 pg/ml. Standard and samples were incubated overnight at 4°C. Plates were washed five times with wash buffer and incubated with polyclonal rabbit anti-mouse IFN-α (PBL Biomedical Laboratories) for 1 h at room temperature. Plates were washed five times and incubated with horseradish peroxidase-conjugated donkey anti-rabbit F(ab)$_2$ (Jackson ImmunoResearch Laboratories) for 1 h at room temperature. Plates were washed 10 times and incubated with 2,2′-azinobis(3-ethylbenzothiazoline-6-sulfonic acid) diammonium salt tablets, 10 mg/tablet (Immunopure ABTS; Pierce), absorbed in 10 ml substrate buffer (1 M acetate buffer, 0.05% Tween 20, pH 4.2). Plates were read at 415 nM absorbance on a Bio-Rad ELISA plate reader.

Isolation of RNA and RT-PCR. Organs obtained as described above were also used to obtain RNA. Lungs were disrupted by using a probe homogenizer in a buffer containing guanidine isothiocyanate, and RNA was isolated following the RNAeasy kit (QIAGEN) instructions. Liver RNA was prepared as previously described (2, 5). Briefly, liver tissue was disrupted using a probe homogenizer in a buffer containing 4.2 M guanidine isothiocyanate, 25 mM Na citrate (pH 7.3), 0.5% sarcosyl, and 100 mM β-mercaptoethanol. The lysate was adjusted to pH 4.0 with 0.1 volume 2 M sodium acetate (pH 4.0), the lysates were extracted twice with a 2.5:1 mixture of phenol (pH 4.0)-chloroform, and RNA was precipitated with an equal volume of isopropanol. The RNA was resuspended in diethylpyrocarbonate-treated H_2O and was further extracted with 1:1 mixture of phenol (pH 8.0)-chloroform. The RNA was precipitated with an equal volume of isopropanol and washed in 80% ethanol. DNA was prepared from 1 μg of RNA by use of random hexamers and a TaqMan RT kit (Applied Biosystems) according to the manufacturer's directions. Real-time reverse transcriptase PCR (RT-PCR) was performed with 5 μl of the RT reaction mixture by using 12.5 μl of SYBR green and 5 μM of forward and reverse primers in a total volume of 25 μl. Primers used are as follows: for IFN-stimulated gene 15 (ISG15), 5′-CAATGGCCTGGGACCTAAA-3′ (sense) and 5′-CTTCTTCAGTTCTGACACCGTCAT-3′ (antisense); for 2′-5′ oligoadenylate synthetase (OAS), 5′-GATGTCAAATCAGCCGTCAA-3′ (sense) and 5′-AGTGTGGTGCCTTTGCCTGA-3′ (antisense); for glyceraldehyde-3-phosphate dehydrogenase (GAPDH), 5′-TCTGGAAAGCTGTGCCGTG-3′ (sense) and 5′-CCAGTGAGCTTCCCGTTCAG-3′ (antisense) (previously described in reference 18); and for TNF-α, 5′-GGGCCACCACGCTCTTCTGTCT-3′ (sense) and 5′-GCCACTCCAGCTGCTCCTCCAC-3′ (antisense) (previously described in reference 13). Real-time PCR was performed with a thermocycler (Applied Biosystems model 7500) using the following program: 50°C for 2 min, 95°C for 10 min, and a 50-cycle repeat of 95°C for 30 s and 60°C for 1 min. All reactions were normalized to GAPDH RNA levels, and induction (*n*-fold) relative to that of samples from uninfected mice was determined by using Applied Biosystems supplied software.

TNF-α bead assay. TNF-α levels were obtained using a cytometric bead assay and a mouse inflammation kit (BD Biosciences) according to the manufacturer's instructions. Briefly, plasma obtained and prepared as described above was used parallel to a supplied standard. Samples or standards were incubated for 2 h at room temperature with mouse inflammation capture beads and phycoerythrin-detecting reagent. Following the incubation, the samples were washed with 1 ml PBS and resuspended in 300 μl PBS. Samples were read by flow cytometry, and concentrations were calculated according to a fluorescence standard mean by using BD CBA software (BD Biosciences) and Microsoft Excel.

Neutralization assay. Neutralization of VSV was performed with mouse serum obtained on day 28 as previously described (17, 22). Neutralizing antibody (nAb) titers are reported as the reciprocal dilution of serum, which gives complete protection of BHK cells from infection with 100 PFU of rwtVSV.

RESULTS

Construction of two ΔM51 viruses. In order to evaluate pathogenicity and immunogenicity of a VSV M mutant lacking the interferon shutoff function, we used site-directed mutagenesis to construct a VSV recombinant with a deletion of the codon for methionine 51 (M51) in the M gene. This deletion was put into two separate recombinant VSV backgrounds, rwtVSV (10) and VSV-EnvG (8). The purpose of the latter construct was to evaluate immunogenicity of the expressed EnvG protein. Both viruses were recovered from plasmid DNAs by use of an established procedure (10).

To confirm expression of the appropriate proteins and the presence of the mutation, we infected cells with the wt and mutant versions of each virus. Cells were labeled with [^{35}S]methionine, and protein lysates were separated by SDS-PAGE. The autoradiograph of the gel is shown in Fig. 1B. All four viruses expressed the five VSV structural proteins: the nucleoprotein (N), the phosphoprotein (P), the matrix protein (M),

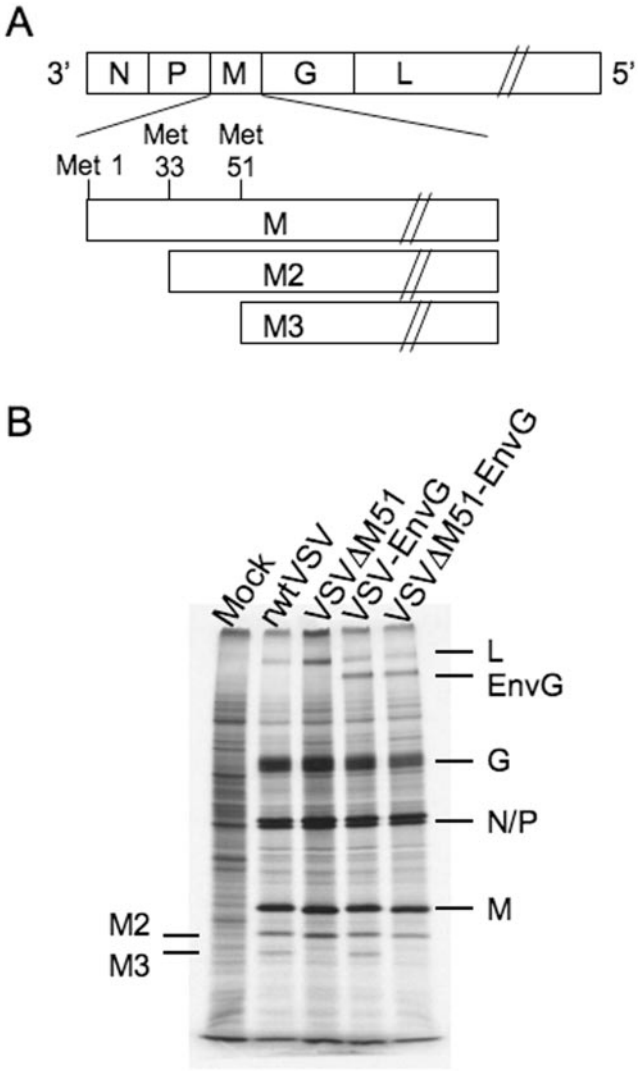

FIG. 1. Viral genome and protein expression. (A) Schematic of the VSV genome, with a diagram indicating the origin of the three VSV M proteins. The M gene encodes the full-length M protein as well as the M2 and M3 proteins, which initiate at the second and third AUG codons in the M mRNA. (B) SDS-PAGE of protein lysates from cells infected with the designated viruses and labeled with [^{35}S]methionine. Positions of VSV and HIV Env proteins are indicated, as are the positions of the internal translational products of M. The gel image was obtained using autoradiography.

the glycoprotein (G), and the RNA-dependent RNA polymerase (L). Cells infected with VSV-EnvG and VSVΔM51-EnvG produced an additional protein, HIV-1 EnvG, of the expected mobility (~145 kDa) (Fig. 1B). Deletion of the codon in the M gene for M51 in VSVΔM51 and VSVΔM51-EnvG viruses also deletes the second of two internal translation start codons (AUGs) in M. These codons, at amino acid positions 33 and 51, are translation initiation sites for two minor proteins, designated M2 and M3, that correspond to N-terminally truncated forms of M protein (Fig. 1A) (7). The loss of the M3 protein from both of the ΔM51 mutants is evident on the gel (Fig. 1B). There is also a small increase in the mobility of the M protein due to loss of the single methionine.

Rapid weight loss following intranasal infection with VSVΔM51 viruses. Intranasal inoculation of mice with rwtVSV results in loss of 15 to 20% of preinfection body weight occurring on days 2 to 4 postinfection (16, 18–20). Attenuated strains of rwtVSV that have truncations in the cytoplasmic domain of G and grow more slowly than rwtVSV cause little or no weight loss in mice after i.n. inoculation (16, 19). Additionally, a VSV recombinant that does not encode G protein and replicates for only a single cycle causes no weight loss in mice after i.n. inoculation (19).

VSV carrying the M51 mutation in M protein was reported to have a greatly reduced 50% lethal dose compared to that of wtVSV in BALB/c mice (26). We initially used weight loss to evaluate the attenuation of a VSVΔM51 mutant following i.n. inoculation (Fig. 2A and B). VSVs expressing the wt M protein (rwtVSV and VSV-EnvG) did not cause weight loss in mice until day 2 after infection, and then the mice continued to lose weight until reaching maximum weight loss at day 4 (16.5% and 11.6% average weight losses, respectively), after which they began to recover. In contrast, we noted that mice infected with VSVΔM51 and VSVΔM51-EnvG lost substantial amounts of weight already in the first day (6.3% and 6.7%, respectively), reached a maximum weight loss at day 2 (7.0% and 7.5%), and then began to recover. Although the maximal weight loss was lower for mice infected with the ΔM51 viruses, the rapid weight loss was unexpected.

Immune responses induced by VSVΔM51-EnvG are reduced. Because the VSVΔM51 infection had an overall attenuated pathology in mice (less total weight loss), we wanted to further evaluate the potential of this virus as an attenuated vaccine vector. We examined the vector's ability to produce a CD8 T-cell response to a foreign protein, HIV Env, by using an established tetramer assay. Seven days post-i.n. or -i.m. infection with VSV-EnvG or VSVΔM51-EnvG, we isolated splenocytes to identify the percentage of CD8 T cells which were activated and HIV Env specific. After i.n. vaccination, we saw a strong response to Env following VSV-EnvG infection (16.1% CD62L^{lo} Env tetramer^{+} CD8 T cells). However, the response to Env post-VSVΔM51-EnvG infection was eightfold less than the response to the VSV-EnvG infection (2.00%). This finding was consistent with many attenuated vectors that induced suboptimal CD8 T-cell response following i.n. vaccination (16, 17).

Other attenuated vectors have induced immune responses comparable to that of the rwt vector when administered via the i.m. route (17; J. Publicover and J. K. Rose, unpublished data). Therefore, we tested the VSVΔM51 vector by the i.m. route. Interestingly, 7 days post-i.m. vaccination, the VSVΔM51 vector elicited a threefold-lower response than the rwtVSV vector (4.9% versus 14.5% CD62L^{lo} Env tetramer^{+} CD8 T cells, respectively). While the threefold difference was less than that observed after i.n. immunization, the VSVΔM51 vector still induced significantly lower primary T-cell responses than the nonattenuated vectors. This difference was not observed with other attenuated vectors given by this route.

Replication and systemic spread of VSVΔM51 is greatly attenuated compared to that of rwtVSV. Following i.n. inoculation, rwtVSV replicates in the mouse lung, causes a transient viremia, and is found transiently in other organs, including liver and spleen (18, 19). To determine if the early weight loss

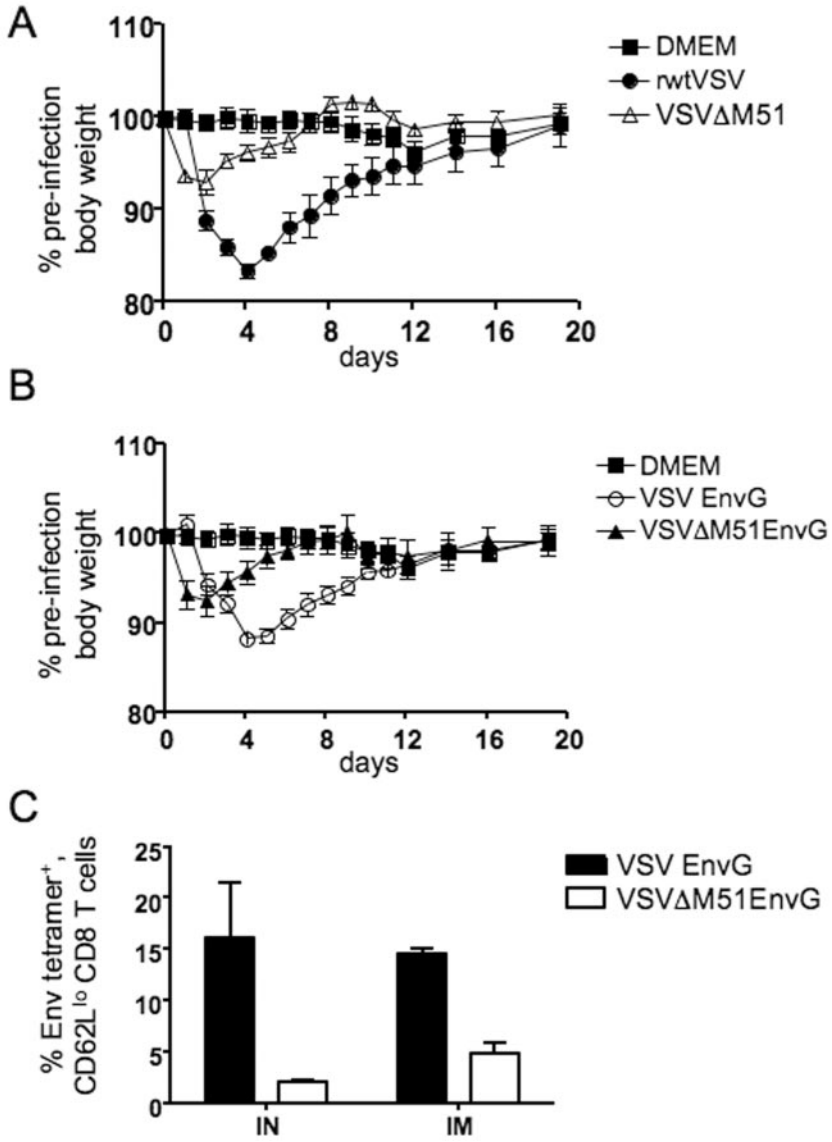

FIG. 2. Weight loss and immune responses induced by VSV recombinants. (A) Weight loss in mice following i.n. infection with rwtVSV or with VSVΔM51 and in control mice given DMEM. (B) Weight loss in mice following infection with VSV-EnvG or VSVΔM51-EnvG or in control mice given DMEM. Error bars represent standard errors of the means ($n = 5$). (C) Percentages of Env-specific (HIV Env tetramer$^+$), activated ($CD62L^{lo}$) $CD8^+$ T-cell responses in spleens, as detected by flow cytometry. Spleens were obtained 7 days after intranasal (IN) or intramuscular (IM) vaccination with VSV-EnvG or VSVΔM51-EnvG. Error bars represent standard errors of the means ($n = 3$).

caused by VSVΔM51 mutants was related to a higher early replication rate, we looked at the VSVΔM51 and rwtVSV titers in the lung, liver, and plasma at various times after i.n. inoculation.

Six hours after i.n. inoculation, the titer of rwt virus in the lung (Fig. 3A) was higher than that of the ΔM51 virus (6.8×10^4 versus 2.1×10^4, respectively). The rwt titers then increased threefold by 12 and 24 h and then fell to about 10^3 PFU/g by 72 h. In contrast, the ΔM51 titers decreased rapidly and were 100-fold below rwt titers by 24 h and undetectable by 72 h. We conclude that the replication of the mutant virus is highly restricted in the lung compared to that of the rwt virus and that faster initial replication cannot explain the rapid weight loss.

We also examined virus titers in the plasma (viremia). Virus appeared in the plasma by 12 h postinfection in five of six mice infected with rwtVSV but in only two of six mice infected with VSVΔM51 (Fig. 3B). By 24 h postinfection, all mice infected with rwtVSV showed a viremia averaging 5.1×10^4 PFU/ml. In contrast, only one of the six mice infected with VSVΔM51 had measurable viremia (1.5×10^2 PFU/ml). By 48 h, three of six rwtVSV-infected mice and all VSVΔM51-infected mice had cleared the virus from the plasma.

We also determined titers of virus in the liver following rwtVSV or VSVΔM51 infection (Fig. 3C). At 24 h postinfection, all mice infected with rwtVSV showed a detectable titer, averaging 10^4 PFU/g. Animals infected with VSVΔM51 did not show a detectable titer in the liver at any time point, consistent with the lack of spread from the lungs.

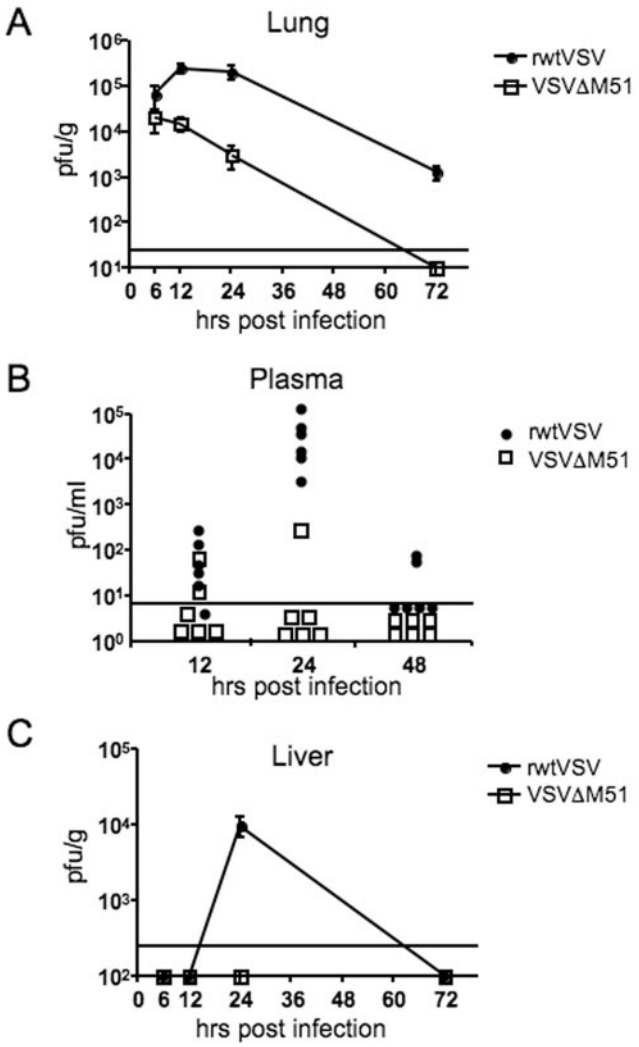

FIG. 3. Viral spread following i.n. infection with rwtVSV or VSVΔM51. Shown are the numbers of PFU of VSV in the lungs (A), plasma (B), and livers (C) of mice infected i.n. with rwtVSV or VSVΔM51 at the designated times postinfection. Titers were determined using a plaque assay with BHK cells. The solid horizontal line shows the limit of sensitivity for the plaque assay (A, 50 PFU; B, 5 PFU; C, 250 PFU). Error bars represent standard errors of the means (A and C, $n = 4$; B, $n = 6$).

Local and systemic interferon production following i.n. inoculation with rwtVSV and VSVΔM51. To determine if i.n. infection by VSVΔM51 induced more interferon synthesis than rwt virus, we monitored the kinetics of IFN-α production early after rwtVSV and VSVΔM51 infection. We measured IFN-α by using an ELISA with plasma and lung supernatants and also measured induction of two IFN-α/β-inducible genes and ISG15 and OAS by using real-time RT-PCR with lung RNA.

Within 6 h postinfection, mice infected with VSVΔM51 showed a strong IFN-α (152.5 pg/ml) response in the lung (Fig. 4A). This response was followed by an increased induction of ISG15 (Fig. 4C) and OAS (Fig. 4D) mRNA expression by 12 h postinfection (64.6 ± 24-fold and 78.9 ± 45.6-fold induction, respectively, compared to results for control mice). IFN-α appeared later in mice infected with rwtVSV, and the levels were never as high as those seen in mice infected with VSVΔM51 (Fig. 4A). The peak induction of IFN-inducible genes following rwtVSV infection was also observed at 24 h and was less than that observed following VSVΔM51 infection (Fig. 4C and D). By 72 h postinfection with either rwtVSV or VSVΔM51, no detectable IFN-α was observed in the lung and the induction of IFN-inducible genes was on the decline (Fig. 4A, C, and D).

IFN-α appeared in the plasma by 24 h, at which time mice infected with rwtVSV had 30-fold-higher levels of IFN-α than VSVΔM51-infected mice (1,350 pg/ml and 44 pg/ml, respectively) (Fig. 4B). Thus, rwtVSV ultimately induces much more IFN systemically than the ΔM51 mutant, presumably because the virus spreads systemically much more efficiently than the mutant.

Rapid induction of TNF-α following VSVΔM51 infection. TNF-α is known to cause weight loss (cachexia) (see references 28 and 29 for a review). Therefore, we wanted to determine if TNF-α was also the mediator of the weight loss we observed in mice following i.n. VSV infection. We measured TNF-α to determine if mice infected with VSVΔM51 showed an early induction of TNF-α. We initially used a real-time RT-PCR assay to measure the increase (*n*-fold) in TNF-α mRNA levels in mice infected with either rwtVSV or VSVΔM51 compared to levels for control, uninfected mice. In the lung at 12 h and 24 h, there was slightly greater induction of TNF-α in VSVΔM51-infected animals than in rwtVSV-infected animals (Fig. 5A). While this increase of TNF-α was not statistically significant, it was consistent throughout infection in the lung. All TNF-α mRNA production was down to background levels by 72 h in mice infected with either virus (Fig. 5A).

At early time points (12 h), we also saw higher plasma levels of TNF-α in VSVΔM51-infected animals than in rwt-infected animals (Fig. 5B) and significantly higher induction of TNF-α mRNA in the liver (Fig. 5C) ($P = 0.0286$). However, at later times the mice infected with rwtVSV had much more TNF-α in the plasma and liver, consistent with the extensive spread of rwt virus. The time course of production of TNF-α in the infected mice was thus consistent with a role in the early weight loss seen with ΔM51-infected animals and the more severe weight loss seen later with rwt-infected animals.

TNF-α knockout mice. To investigate further the potential role of TNF-α in weight loss after VSV infection, we chose to examine the pathogenesis of rwtVSV and VSVΔM51 in TNF-α knockout (TNF-$\alpha^{-/-}$) mice (14). Because these mice are available only on a C57BL/6 background, we used C57BL/6 mice as controls. We inoculated age- and sex-matched TNF-$\alpha^{-/-}$ or control mice with rwtVSV, VSVΔM51, or DMEM, and mice were then weighed daily.

Following infection of wild-type mice with rwtVSV, we observed the first weight loss on day 2 (7.3% of preinfection body weight) (Fig. 6A); this weight loss continued to day 3 (9.0%), followed by a gradual recovery to the original weight by day 8. Infection of TNF-$\alpha^{-/-}$ mice by rwt virus resulted in significantly less weight loss, only 2.3% through days 2 and 3 ($P = 0.0159$), and then a full recovery by day 5. These results are consistent with a role of TNF-α in causing weight loss following rwtVSV infection.

In contrast to what we saw with the BALB/c background mice, infection of wild-type C57BL/6 mice with VSVΔM51 resulted in only 1.5% weight loss on day 1, followed by a

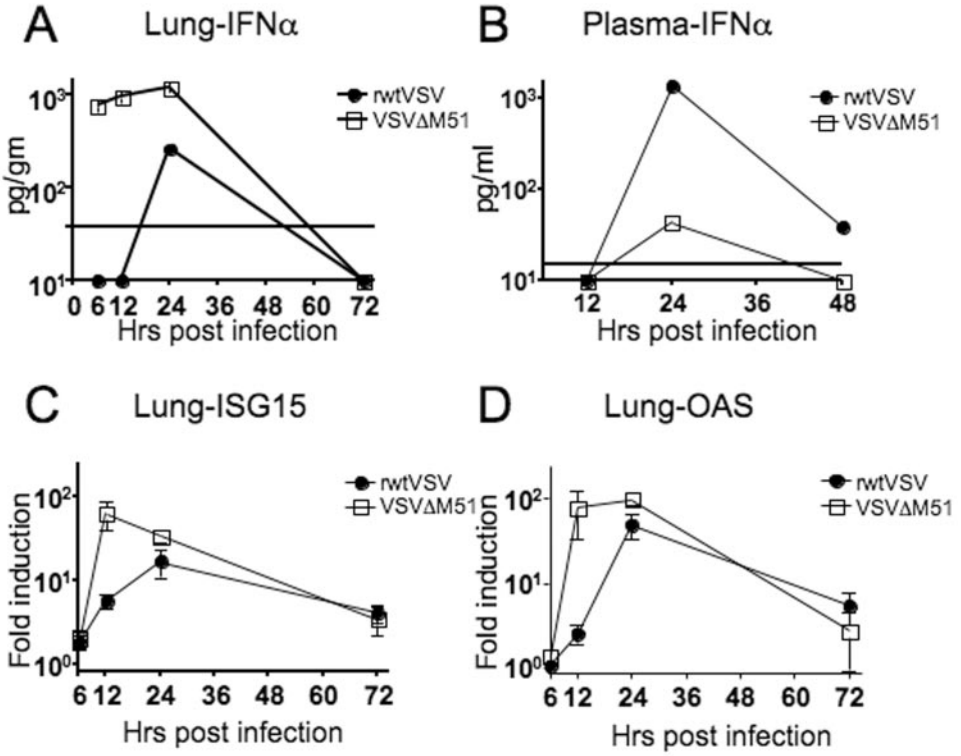

FIG. 4. Induction of IFN-α- and IFN-α/β-inducible genes in rwtVSV- or VSVΔM51-infected mice. (A and B) IFN-α response, detected by ELISA, in lung supernatants (A) or plasma (B) at the designated times following i.n. infection of mice with rwtVSV or VSVΔM51. The solid horizontal line indicates the limit of sensitivity of the ELISA (A, 38 pg; B, 15.2 pg). Any numbers on the baseline indicate values below these limits of detection. Plasma and lung supernatant samples were pooled from six or four mice, respectively, at each time point. (C and D) Induction of ISG15 (C) or OAS (D) in mRNA from lungs, determined by real-time RT-PCR. ISG15 and OAS gene levels were normalized to GAPDH levels and are reported as increases (*n*-fold) in induction over levels for DMEM-administered controls. Error bars represent standard errors of the means ($n = 4$).

recovery to above 100% by day 2 (Fig. 6B). However, infection of TNF-$\alpha^{-/-}$ mice with VSVΔM51 was followed by a weight gain of 2.7% on day 1. Thus, although rapid weight loss following ΔM51 infection was less pronounced in C57BL/6 mice, all weight loss was abolished in the absence of TNF-α and, in fact, was replaced by a weight gain. The difference in weight change between the C57BL/6 mice and the TNF-α knockout mice on day 1 was statistically significant ($P = 0.0159$). Mock-infected control mice remained above 100% preinfection body weight at all times (Fig. 6C).

TNF-$\alpha^{-/-}$ mice are infected by VSV. To be certain that lack of TNF-α had not caused mice to somehow become refractory to VSV infection, we first examined virus titer and IFN-α induction at 24 h post-rwtVSV infection. At this time, both TNF-$\alpha^{-/-}$ and C57BL/6 mice showed a high viremia (7.9×10^4 PFU/ml and 8.1×10^4 PFU/ml, respectively) and produced large amounts of IFN-α (2,201 pg/ml and 1,849 pg/ml, respectively), indicating that infection had indeed occurred (Fig. 6D and E). Additionally, we examined nAb levels to VSV produced 28 days postinfection in rwtVSV- and VSVΔM51-infected TNF-$\alpha^{-/-}$ knockout mice (Fig. 6F). Both C57BL/6 and TNF-$\alpha^{-/-}$ mice produced comparable VSV nAb titers following rwtVSV (4,096 ± 627 and 5,632 ± 1,254, respectively) and VSVΔM51 (4,480 ± 640 and 3,840 ± 809, respectively) infection. Because infection must occur for induction of VSV nAb or IFN-α (19; Publicover and Rose, unpublished), we conclude that the lack of weight loss following infection in the TNF-$\alpha^{-/-}$ background was not due to differences in IFN-α production or absence of infection.

DISCUSSION

Because VSV replication is entirely cytoplasmic, VSV can inhibit host responses to infection by blocking mRNA transport from the nucleus to the cytoplasm. VSV M protein, in addition to being a major viral structural protein, mediates this transport block and thereby inhibits interferon production in infected cells (4, 6, 15). VSV M proteins with mutations at methionine 51 do not inhibit host mRNA transport and allow interferon production in infected cells (4, 15, 26, 30). VSV mutants carrying such mutations have a higher 50% lethal dose, induce more interferon, and replicate to lower titers in infected mice (26). Here we report an unexpected, rapid weight loss pathology following intranasal infection of mice with such an M mutant. This rapid weight loss (7% of body weight in the BALB/c background) occurred largely in the first 24 h following infection, a time period when mice infected with rwtVSV do not show any weight loss. Instead, mice infected with rwtVSV show greater weight loss, 15 to 17% of body weight, occurring later, between 24 and 96 h following infection.

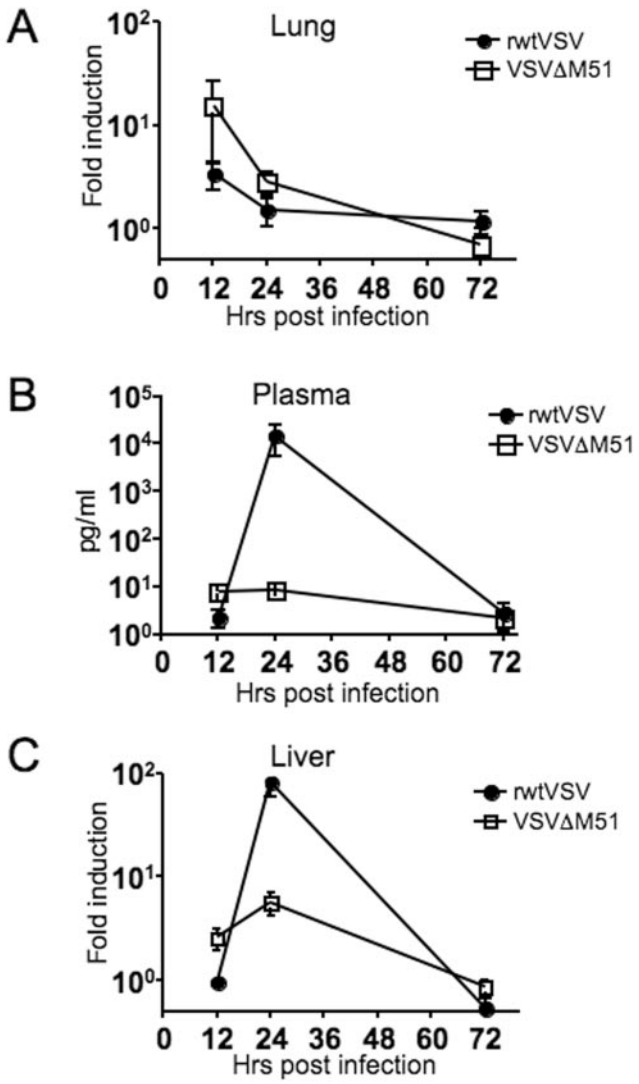

FIG. 5. TNF-α levels in mice following i.n. infection with rwtVSV or VSVΔM51. (A) Induction of TNF-α in lung mRNA, measured by real-time RT-PCR. TNF-α gene levels were normalized to GAPDH levels and are reported as increases (*n*-fold) in induction over levels for DMEM-administered controls. (B) Concentration of TNF-α in the plasma at the given time points postinfection. TNF-α was measured using a cytometric bead assay (BD Biosciences) and analyzed by flow cytometry. (C) Induction of TNF-α in liver mRNA, measured by real-time RT-PCR. TNF-α gene levels were normalized to GAPDH levels and are reported as increases (*n*-fold) in induction over levels for DMEM-administered controls. Error bars for all panels represent standard errors of the means ($n = 4$).

VSV given intranasally to mice replicates in the lungs, causes a transient viremia, and then spreads systemically to other organs (18, 19). In contrast, we found that the VSVΔM51 mutant replicated poorly in the lungs and generated little or no viremia or spread to other organs. We also found that the mutant induced much more interferon in the lungs than rwtVSV. VSV replication is very sensitive to interferon, and therefore this rapid induction of interferon, likely originating in infected cells, could easily explain the control of mutant virus replication. Conversely, the rwtVSV infection is able to block IFN production in infected cells, allowing replication to occur at the site of infection in the absence of IFN responses. This infection eventually leads to a viremia and extensive spread of virus to other organs.

Although IFN induction is not associated with rapid weight loss, another cytokine, TNF-α (previously known as cachectin), is a well-established mediator of toxic shock and weight loss (cachexia) (1, 28, 29). Because viral infections can lead to induction of TNF-α and weight loss in mice (for an example, see reference 23), we examined synthesis of TNF-α in mice infected with the rwt and mutant viruses. We found an earlier induction of TNF-α in mice infected with VSVΔM51, correlating with earlier weight loss. The later and greater weight loss in mice infected with rwtVSV correlated with much higher levels of TNF-α production later in infection when the viral infection had become systemic. A role for TNF-α in weight loss induced by VSV infection was also established with TNF-$\alpha^{-/-}$ mice. These mice showed little or no weight loss following infection by either rwtVSV or VSVΔM51.

While we show here that TNF-α likely mediates much of the weight loss pathology for VSV-infected mice, we did observe a low-level weight loss with rwtVSV-infected TNF-α knockout mice. It is therefore likely that other factors, potentially including other inflammatory cytokines, contribute to the weight loss pathology. For example, we have seen a time course of interleukin-6 production similar to that of TNF-α production in the plasma of mice infected with rwtVSV and ΔM51 viruses (data not shown), and interleukin-6 production contributes to weight loss following influenza infection (9).

We do not know the types of cells infected by VSV in the lungs or elsewhere in the mouse following intranasal infection. Whatever cells are infected, it appears likely that the VSVΔM51 mutant induces more IFN synthesis in those cells than does rwt virus, because it fails to shut off nuclear export of induced IFN mRNA. A similar mechanism might apply for increased synthesis of TNF-α if its synthesis is also induced in VSV-infected cells. There is one report of induction of TNF-α synthesis in HL-60 cells (a promyelomonocyte cell line) following VSV infection (31). Additionally, there are reports that influenza and adenovirus infection of alveolar macrophages, resident in the respiratory tract, result in TNF-α production (25, 32).

We observed previously that expression of HIV EnvG from the rwt vector decreased the weight loss normally induced by the rwtVSV between 24 and 96 h (16). This effect is apparent in Fig. 2A and B. This attenuating effect is likely due to slowing of virus replication by the expression of HIV Env. Interestingly, inclusion of EnvG had no effect on the rapid, early weight loss induced by the VSVΔM51 mutant (Fig. 2A and B). We also examined the effect of the ΔM51 mutation in the background of an attenuated VSV mutant that has a G protein with its cytoplasmic tail truncated from 29 to 9 amino acids (VSVGCT9). The VSVGCT9 virus causes little or no weight loss in mice (16), apparently because of very limited replication. However, the VSVGCT9 ΔM51 double mutant caused rapid, early weight loss (data not shown). Thus, the ΔM51 mutation has a dominant effect in causing rapid weight loss in the presence of mutations that would eliminate or attenuate weight loss in the wild-type background by reducing viral spread. The likely explanation for this dominance is that the

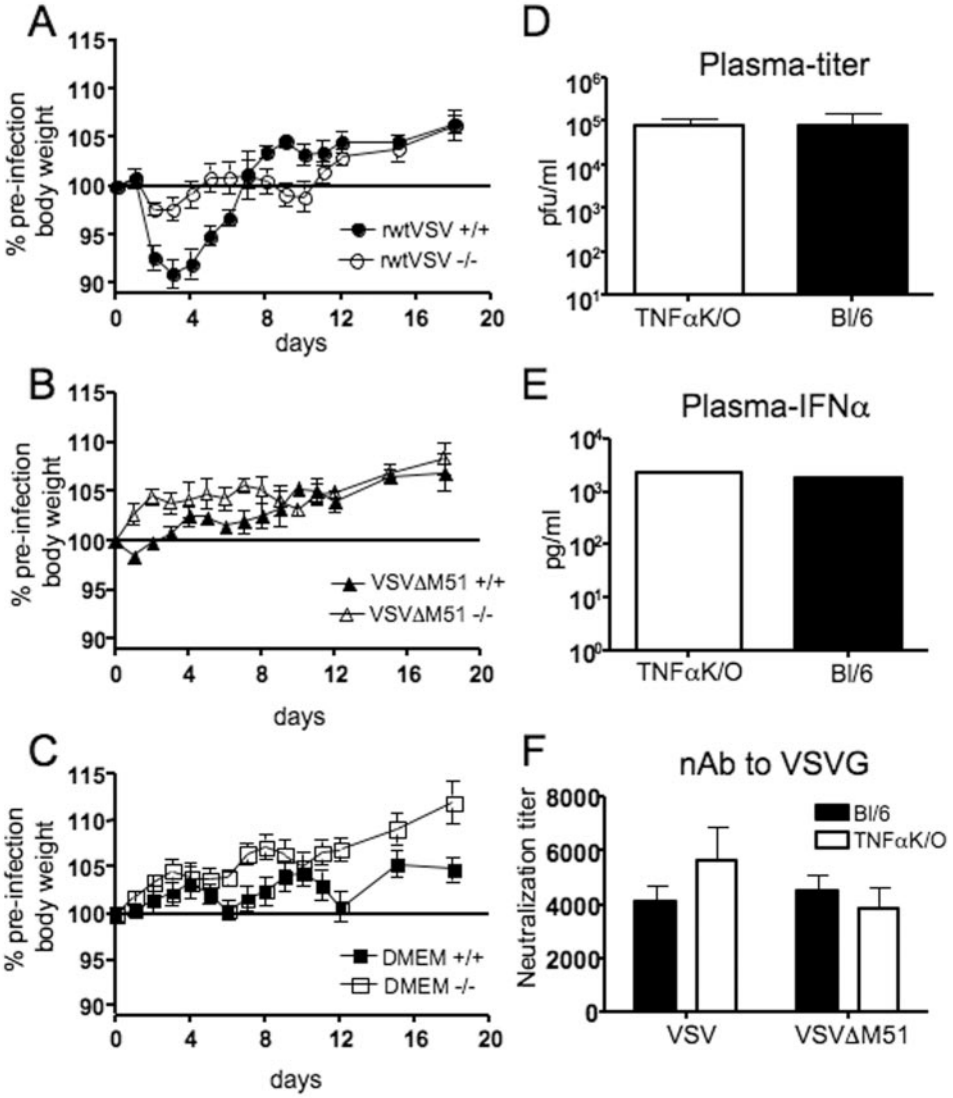

FIG. 6. rwtVSV and VSVΔM51 pathology in knockout (K/O) mice. (A) Weight loss in C57BL/6 (+/+, filled circles) or TNF-α K/O (−/−, open circles) mice following i.n. infection with rwtVSV. Error bars represent standard errors of the means ($n = 5$). (B) Weight loss in C57BL/6 (+/+, filled triangles) or TNF-α K/O (−/−, open triangles) mice following i.n. infection with VSVΔM51. Error bars represent standard errors of the means ($n = 5$). (C) Weight loss in mock-infected control C57BL/6 (+/+, filled squares) or TNF-α K/O (−/−, open squares) mice following i.n. administration of DMEM. Error bars represent standard errors of the means ($n = 5$). (D) Viral titers in plasma 24 h post-rwtVSV infection in C57BL/6 and TNF-α K/O mice. Error bars represent standard errors of the means ($n = 3$). (E) IFN-α levels, obtained by ELISA, in mouse plasma 24 h post-rwtVSV infection in C57BL/6 and TNF-α K/O mice. Plasma was pooled from three mice. (F) nAb titers to VSV G in sera of C57BL/6 and TNF-α K/O mice 28 days postinfection with rwtVSV. Error bars represent standard errors of the means ($n = 3$).

effect of the ΔM51 mutation occurs in the primary infected cells and does not require spread beyond these cells.

We also compared the CD8 T-cell responses to HIV Env induced by the VSVΔM51-EnvG vector and the VSV-EnvG vector. We found that the responses to EnvG were reduced three- to eightfold in the ΔM51 background. Interestingly, the same reduction was seen after either i.n. or i.m. inoculation. This result was surprising because other attenuated VSV vectors capable of only a single cycle of replication or vectors replicating poorly due to G cytoplasmic-tail truncations induce poor responses when given intranasally but strong responses equivalent to those induced by rwtVSV when given intramuscularly (16, 17; Publicover and Rose, unpublished). The equivalent responses generated by single-cycle vectors given i.m. suggested that maximal immune responses are generated by replication only in the primary infected cells after i.m. inoculation. The lower response generated by the ΔM51 virus given i.m. implies lower level primary replication, likely due to rapid induction of interferon in infected cells.

It should be noted that there is no induction of weight loss by rwtVSV given intranasally to rhesus macaques (21) or guinea pigs (12). Weight loss is therefore clearly a species-specific phenomenon and even differs among mouse strains. This effect presumably depends on the amount of viral replication and the extent of cytokine induction. The ΔM51 mutant has not yet been tested with nonhuman primates or guinea pigs.

ACKNOWLEDGMENTS

This work was supported by NIH grants R37-AI40357 to J.K.R. and K22-AI064757 to M.R. and by HVDDT contract NO1-AI25458.

REFERENCES

1. **Cerami, A., and B. Beutler.** 1988. The role of cachectin/TNF in endotoxic shock and cachexia. Immunol. Today **9:**28–31.
2. **Chomczynski, P., and N. Sacchi.** 1987. Single-step method of RNA isolation by acid guanidinium thiocyanate-phenol-chloroform extraction. Anal. Biochem. **162:**156–159.
3. **de Mattos, C. A., C. C. de Mattos, and C. E. Rupprecht.** 2001. Rhabdoviruses, p. 1245–1278. *In* D. M. Knipe, P. M. Howley, D. E. Griffin, R. A. Lamb, M. A. Martin, B. Roizman, and S. E. Straus (ed.), Fields virology, 4th ed., vol. 2. Lippincott Williams & Wilkins, Philadelphia, Pa.
4. **Faria, P. A., P. Chakraborty, A. Levay, G. N. Barber, H. J. Ezelle, J. Enninga, C. Arana, J. van Deursen, and B. M. Fontoura.** 2005. VSV disrupts the Rae1/mrnp41 mRNA nuclear export pathway. Mol. Cell **17:**93–102.
5. **Guidotti, L. G., B. Matzke, H. Schaller, and F. V. Chisari.** 1995. High-level hepatitis B virus replication in transgenic mice. J. Virol. **69:**6158–6169.
6. **Her, L. S., E. Lund, and J. E. Dahlberg.** 1997. Inhibition of Ran guanosine triphosphatase-dependent nuclear transport by the matrix protein of vesicular stomatitis virus. Science **276:**1845–1848.
7. **Jayakar, H. R., and M. A. Whitt.** 2002. Identification of two additional translation products from the matrix (M) gene that contribute to vesicular stomatitis virus cytopathology. J. Virol. **76:**8011–8018.
8. **Johnson, J. E., M. J. Schnell, L. Buonocore, and J. K. Rose.** 1997. Specific targeting to $CD4^+$ cells of recombinant vesicular stomatitis viruses encoding human immunodeficiency virus envelope proteins. J. Virol. **71:**5060–5068.
9. **Kozak, W., V. Poli, D. Soszynski, C. A. Conn, L. R. Leon, and M. J. Kluger.** 1997. Sickness behavior in mice deficient in interleukin-6 during turpentine abscess and influenza pneumonitis. Am. J. Physiol. **272:**R621–R630.
10. **Lawson, N. D., E. A. Stillman, M. A. Whitt, and J. K. Rose.** 1995. Recombinant vesicular stomatitis viruses from DNA. Proc. Natl. Acad. Sci. USA **92:**4477–4481.
11. **Lund, J. M., L. Alexopoulou, A. Sato, M. Karow, N. C. Adams, N. W. Gale, A. Iwasaki, and R. A. Flavell.** 2004. Recognition of single-stranded RNA viruses by Toll-like receptor 7. Proc. Natl. Acad. Sci. USA **101:**5598–5603.
12. **Natuk, R. J., D. Cooper, M. Guo, P. Calderon, K. J. Wright, F. Nasar, S. Witko, D. Pawlyk, M. Lee, J. Destefano, D. Tummolo, A. S. Abramovitz, S. Gangolli, N. Kalyan, D. K. Clarke, R. M. Hendry, J. H. Eldridge, S. A. Udem, and J. Kowalski.** 2006. Recombinant vesicular stomatitis virus vectors expressing herpes simplex virus type 2 gD elicit robust $CD4^+$ Th1 immune responses and are protective in mouse and guinea pig models of vaginal challenge. J. Virol. **80:**4447–4457.
13. **Ouyang, X., T. H. Le, C. Roncal, C. Gersch, J. Herrera-Acosta, B. Rodriguez-Iturbe, T. M. Coffman, R. J. Johnson, and W. Mu.** 2005. Th1 inflammatory response with altered expression of profibrotic and vasoactive mediators in AT1A and AT1B double-knockout mice. Am. J. Physiol. Renal Physiol. **289:**F902–F910.
14. **Pasparakis, M., L. Alexopoulou, V. Episkopou, and G. Kollias.** 1996. Immune and inflammatory responses in TNF alpha-deficient mice: a critical requirement for TNF alpha in the formation of primary B cell follicles, follicular dendritic cell networks and germinal centers, and in the maturation of the humoral immune response. J. Exp. Med. **184:**1397–1411.
15. **Petersen, J. M., L. S. Her, V. Varvel, E. Lund, and J. E. Dahlberg.** 2000. The matrix protein of vesicular stomatitis virus inhibits nucleocytoplasmic transport when it is in the nucleus and associated with nuclear pore complexes. Mol. Cell. Biol. **20:**8590–8601.
16. **Publicover, J., E. Ramsburg, and J. K. Rose.** 2004. Characterization of nonpathogenic, live, viral vaccine vectors inducing potent cellular immune responses. J. Virol. **78:**9317–9324.
17. **Publicover, J., E. Ramsburg, and J. K. Rose.** 2005. A single-cycle vaccine vector based on vesicular stomatitis virus can induce immune responses comparable to those generated by a replication-competent vector. J. Virol. **79:**13231–13238.
18. **Ramsburg, E., J. Publicover, L. Buonocore, A. Poholek, M. Robek, A. Palin, and J. K. Rose.** 2005. A vesicular stomatitis virus recombinant expressing granulocyte-macrophage colony-stimulating factor induces enhanced T-cell responses and is highly attenuated for replication in animals. J. Virol. **79:**15043–15053.
19. **Roberts, A., L. Buonocore, R. Price, J. Forman, and J. K. Rose.** 1999. Attenuated vesicular stomatitis viruses as vaccine vectors. J. Virol. **73:**3723–3732.
20. **Roberts, A., and J. K. Rose.** 1998. Recovery of negative-strand RNA viruses from plasmid DNAs: a positive approach revitalizes a negative field. Virology **247:**1–6.
21. **Rose, N. F., P. A. Marx, A. Luckay, D. F. Nixon, W. J. Moretto, S. M. Donahoe, D. Montefiori, A. Roberts, L. Buonocore, and J. K. Rose.** 2001. An effective AIDS vaccine based on live attenuated vesicular stomatitis virus recombinants. Cell **106:**539–549.
22. **Rose, N. F., A. Roberts, L. Buonocore, and J. K. Rose.** 2000. Glycoprotein exchange vectors based on vesicular stomatitis virus allow effective boosting and generation of neutralizing antibodies to a primary isolate of human immunodeficiency virus type 1. J. Virol. **74:**10903–10910.
23. **Rutigliano, J. A., and B. S. Graham.** 2004. Prolonged production of TNF-alpha exacerbates illness during respiratory syncytial virus infection. J. Immunol. **173:**3408–3417.
24. **Schnell, M. J., L. Buonocore, M. A. Whitt, and J. K. Rose.** 1996. The minimal conserved transcription stop-start signal promotes stable expression of a foreign gene in vesicular stomatitis virus. J. Virol. **70:**2318–2323.
25. **Seo, S. H., R. Webby, and R. G. Webster.** 2004. No apoptotic deaths and different levels of inductions of inflammatory cytokines in alveolar macrophages infected with influenza viruses. Virology **329:**270–279.
26. **Stojdl, D. F., B. D. Lichty, B. R. tenOever, J. M. Paterson, A. T. Power, S. Knowles, R. Marius, J. Reynard, L. Poliquin, H. Atkins, E. G. Brown, R. K. Durbin, J. E. Durbin, J. Hiscott, and J. C. Bell.** 2003. VSV strains with defects in their ability to shutdown innate immunity are potent systemic anti-cancer agents. Cancer Cell **4:**263–275.
27. **Tesh, R. B., P. H. Peralta, and K. M. Johnson.** 1969. Ecologic studies of vesicular stomatitis virus. I. Prevalence of infection among animals and humans living in an area of endemic VSV activity. Am. J. Epidemiol. **90:**255–261.
28. **Tracey, K. J.** 2002. Lethal weight loss: the focus shifts to signal transduction. Sci. STKE **2002:**PE21.
29. **Tracey, K. J., and A. Cerami.** 1993. Tumor necrosis factor, other cytokines and disease. Annu. Rev. Cell Biol. **9:**317–343.
30. **von Kobbe, C., J. M. van Deursen, J. P. Rodrigues, D. Sitterlin, A. Bachi, X. Wu, M. Wilm, M. Carmo-Fonseca, and E. Izaurralde.** 2000. Vesicular stomatitis virus matrix protein inhibits host cell gene expression by targeting the nucleoporin Nup98. Mol. Cell **6:**1243–1252.
31. **Wong, G. H., and D. V. Goeddel.** 1986. Tumour necrosis factors alpha and beta inhibit virus replication and synergize with interferons. Nature **323:**819–822.
32. **Zsengeller, Z., K. Otake, S. A. Hossain, P. Y. Berclaz, and B. C. Trapnell.** 2000. Internalization of adenovirus by alveolar macrophages initiates early proinflammatory signaling during acute respiratory tract infection. J. Virol. **74:**9655–9667.